Fourteenth European Rotorcraft Forum

Paper No. 55

IDENTIFICATION OF A COUPLED FLAPPING/INFLOW MODEL FOR THE PUMA HELICOPTER FROM FLIGHT TEST DATA

Ronald Du Val, Ofer Bruhis and John Green

Advanced Rotorcraft Technology, Inc
Mountain View, California

20 – 23 September, 1988
Milano, ITALY

Associazione Industrie Aerospaziali
Associazione Italiana di Aeronautica ed Astronautica

Introduction

Linear mathematical models providing functional representations of rotorcraft dynamics are commonly used for stability and control or handling qualities applications. Such linear models are either obtained numerically from simulations using physically based nonlinear math models or identified directly from flight test data. The former approach is far less costly than the latter but requires that the physically based nonlinear math model first be validated across the required flight envelope. While such a validation effort is far more difficult than direct identification of linear functional models from flight test data, it can conceivably be accomplished with fewer test points and thereby reduce the cost of the required flight test program. It would also provide a systematic approach for correlation of theoretical and experimental results obtained from a variety of rotorcraft investigations.

Under the Technical Cooperation Program (TTCP), an international effort has been initiated to evaluate the use of state-of-the-art system identification methodology for validating and/or upgrading physically based mathematical models used in comprehensive rotorcraft simulations. A recent Workshop in this program was held in Bedford, England in March 1988 with the specific objective of using modern system identification methods to validate a physically based model of coupled rotor cyclic flapping/first harmonic inflow dynamics from Puma flight test data provided by the Royal Aeronautical Establishment (RAE). This paper describes the results obtained by Advanced Rotorcraft Technology, Inc. in supporting the TTCP-HTP 6 System Identification Workshop in Bedford.

Objectives

The primary objective of this study was to evaluate the use of modern system identification methodology to validate physically based mathematical models from experimental flight test data. Most recent work in helicopter parameter identification has concentrated on the identification of stability and control derivatives of a linear model of specified order. This is essentially a curve fitting problem in which a functional representation of input/output data is specified and the parameter values that provide the best match to experimental data is determined. The validation of a physically based math model is far more difficult since both the model structure and the parameters must be determined. The physical model chosen to evaluate this methodology is a coupled rotor flapping/inflow dynamics model. The baseline structure of this model was taken from the literature [Ref. 1 and 2] and is representative of the technology used in nonlinear flight simulations for stability and control and handling qualities work. A secondary objective of this study is to validate the structure of this model and estimate values for the parameters of the model.

Approach

The following steps were carried out to accomplish the objectives of this study.

1) *Establish structure of baseline math model.* After reviewing the literature, a baseline model was chosen to reflect generally accepted technology. The rotor dynamics model was based on the work of Chen [Ref.1] with modifications made to account for the French rotation of the Puma Helicopter and the inclusion of first harmonic

[Ref.2] with a Glauert model of the quasistatic, velocity dependent first harmonic inflow.

2) *Perform consistency tests on flight test data.* Since the test data was to be used to validate the math model, it was essential that the data be consistent. A series of comparisons of redundant sensors and sensors that can be compared through known kinematic relationships was used to eliminate sensor biases and isolate faulty measurements.
3) *Establish consistency of model structure with flight test data.* Having established the consistency of the flight test data, the validity of the baseline model structure was tested by examining the equation error resulting from applying the test data to the baseline model for a nominal set of model parameter values. The baseline model structure was then extended as required to assure consistency.
4) *Identify parameters of model from flight test data.* An output error parameter identification method was used to identify selected parameters of the validated model structure. The technique was first tested using simulated data generated from the baseline model. It was then applied to the lateral maneuver at 130 knots and a set of ten parameters were identified. These parameters were then used with the model to predict the response for the longitudinal maneuver and the results were compared with flight test data to validate the parameters.

Cyclic Flapping/First Harmonic Inflow Math Model

It was decided to use an isolated model of coupled rotor/inflow dynamics rather than a fully coupled rotor fuselage dynamics model. This approach of dealing with isolated subsets of the total system allows for a systematic validation of each subsystem independently and reduces the complexity of each model to a manageable level. In order to isolate the mathematical model of a subsystem, the variables involved in cross coupling with other subsystems are treated as measured inputs to the isolated subsystem.

The cyclic flapping model is based on Chen's work [Ref. 1]. It is a two degree of freedom model with second order dynamics and has been modified to account for the French rotation of the Puma and to include first harmonic inflow components. The dynamics of the longitudinal and lateral flapping states (a_{1s} and b_{1s}) are driven by the longitudinal and lateral cyclic pitch controls (B_1 and A_1), dynamic first harmonic inflow (p_i and q_i) and a quasistatic first harmonic inflow based on advance ratios (μ_x and μ_y). The cyclic inflow dynamics is also driven by the roll and pitch rates (p and q) and nonlinear functions (u_a and u_b) of coning angle and coning angle rate (a_0 and $\dot{a}_0$), uniform inflow (λ_c), collective pitch (θ_0), and advance ratio (μ). The baseline model has the form:

$$\begin{bmatrix} \ddot{a}_{1s} \\ \ddot{b}_{1s} \end{bmatrix} + F_1 \begin{bmatrix} \dot{a}_{1s} \\ \dot{b}_{1s} \end{bmatrix} + F_2 \begin{bmatrix} a_{1s} \\ b_{1s} \end{bmatrix} = G_1 \begin{bmatrix} A_1 \\ B_1 \end{bmatrix} + G_2 \begin{bmatrix} p_i \\ q_i \end{bmatrix} + +G_3 \begin{bmatrix} p \\ q \end{bmatrix} + \begin{bmatrix} u_a \\ u_b \end{bmatrix} \quad (1)$$

where

$$u_a = \frac{1}{2}\gamma\Omega^2 a_0 \mu_x B_{32} + \gamma\Omega^2 \theta_0 \mu_y B_{32} + \frac{1}{2}\gamma\Omega^2 \lambda_c \mu_y B_{21} + \frac{1}{2}\gamma\Omega^2 \dot{a}_0 \mu_y B_{32} \quad (2)$$

$$u_b = \frac{1}{2}\gamma\Omega^2 a_0 \mu_y B_{32} - \gamma\Omega^2 \theta_0 \mu_x B_{32} - \frac{1}{2}\gamma\Omega^2 \lambda_c \mu_x B_{21} - \frac{1}{2}\gamma\Omega^2 \dot{a}_0 \mu_x B_{32}$$

and

$$F_1 = \begin{bmatrix} \frac{1}{2}\gamma\Omega(B_{43} - b_{32}\epsilon_1) & 2\Omega \\ -2\Omega & \frac{1}{2}\gamma\Omega(B_{43} - b_{32}\epsilon_1) \end{bmatrix}$$

$$F_2 = \begin{bmatrix} \epsilon_\beta\Omega^2 - \frac{1}{4}\gamma\Omega^2\mu_x\mu_y B_{21} & \frac{1}{2}\gamma\Omega^2(B_{43} - B_{32}\epsilon_1 + \frac{1}{4}(\mu_x^2 - \mu_y^2)B_{21}) \\ -\frac{1}{2}\gamma\Omega^2(B_{43} - B_{32}\epsilon_1 - \frac{1}{4}(\mu_x^2 - \mu_y^2)B_{21}) & \epsilon_\beta\Omega^2 - \frac{1}{4}\gamma\Omega^2\mu_x\mu_y B_{21} \end{bmatrix}$$

$$G_1 = \begin{bmatrix} \frac{1}{2}\gamma\Omega^2(B_{43} + \frac{1}{4}\mu_x^2 B_{21} - \frac{1}{4}\mu_y^2 B_{21}) & \frac{1}{4}\gamma\Omega^2\mu_x\mu_y B_{21} \\ \frac{1}{4}\gamma\Omega^2\mu_x\mu_y B_{21} & \frac{1}{2}\gamma\Omega^2(B_{43} - \frac{1}{4}\mu_x^2 B_{21} + \frac{1}{4}\mu_y^2 B_{21}) \end{bmatrix} \tag{3}$$

$$G_2 = \begin{bmatrix} 0 & \frac{1}{2}\gamma\Omega B_{43} \\ \frac{1}{2}\gamma\Omega B_{43} & 0 \end{bmatrix}$$

$$G_3 = \begin{bmatrix} 2\Omega(1+\epsilon_\beta) & -\frac{1}{2}\gamma\Omega B_{43} \\ \frac{1}{2}\gamma\Omega B_{43} & 2\Omega(1+\epsilon_\beta) \end{bmatrix}$$

The uncertain parameters are the Lock Number (γ), and the Tip Loss Factor, (B), where

$$B_{43} \approx \frac{B^4}{4} - \frac{B^3}{3}e, \qquad B_{32} \approx \frac{B^3}{3} - \frac{B^2}{2}e, \qquad B_{21} \approx \frac{B^2}{2} - Be$$

and e is defined as the nondimensional hinge offset.

The inflow model is based on the work of Peters [Ref. 2]. It is a two degree of freedom model with first order dynamics and is given by:

$$\begin{bmatrix} \dot{p}_i \\ \dot{q}_i \end{bmatrix} + F_3 \begin{bmatrix} p_i \\ q_i \end{bmatrix} = G_4 \left(\begin{bmatrix} p \\ q \end{bmatrix} - \begin{bmatrix} 0 & \Omega \\ \Omega & 0 \end{bmatrix} \begin{bmatrix} A_1 - b_{1s} \\ B_1 + a_{1s} \end{bmatrix} + \begin{bmatrix} \dot{a}_{1s} \\ \dot{b}_{1s} \end{bmatrix} \right) \tag{4}$$

where

$$F_3 = \begin{bmatrix} \frac{1}{\tau} & 0 \\ 0 & \frac{1}{\tau} \end{bmatrix}, \qquad G_4 = \begin{bmatrix} k & 0 \\ 0 & k \end{bmatrix} \tag{5}$$

The uncertain parameters are the inflow time constant (τ), and the gain on the forcing function (k). The equations are linearized about the trimmed condition to further simplify the relationship. This results in the elimination of the nonlinear forcing functions (u_a and u_b) since there is little variation in their variables. Equations 1) through 5) otherwise remain the same except that the states are now interpreted as perturbations from the trim condition.

Consistency Tests of Flight Test Data

The flight test data utilized was provided by the Royal Aeronautical Establishment (RAE) and consisted of longitudinal and lateral doublets for the Puma helicopter at 130 knots. The longitudinal maneuver was used for identification since it provided significantly more excitation in both axes than the lateral maneuver. Available sensors

include flapping and feathering sensors on each blade, blade 1 azimuth, body axis velocity sensors, rates and attitudes. Harmonic analysis was applied to the flapping data from each blade to obtain redundant estimates of the longitudinal and lateral tip path plane angles and the coning angle. The data windows for harmonic analysis were sufficiently short that the rotor dynamics could be accurately tracked. Figure 1 shows a comparison of the time histories of longitudinal and lateral flapping dynamics as obtained from harmonic analysis of different blades. The close comparison demonstrates the consistency of the data. Figure 2 shows a comparison of measured pitch attitude with the integral of pitch rate. This kinematic constraint demonstrates the presence of a bias in the pitch rate measurement. The third curve in Figure 2 shows that the integral of pitch rate with the estimated bias removed matches the pitch attitude well. Figure 3 shows time histories of control inputs, body rates, velocity components, coning angle and coning angle rate for the longitudinal doublet maneuver. These variables are all inputs to the isolated model of coupled cyclic flapping /first harmonic inflow dynamics.

Consistency of Model with Flight Test Data

Having validated the test data, the validity of the baseline model structure is next evaluated. It is essential to validate the model structure prior to identifying parameters. If the model structure is incorrect, parameters may still be identified that track the data accurately, but the parameter values will be physically meaningless. The inflow equation is first integrated, using nominal parameter values and the measured time histories of forcing functions. The resulting inflow time history is then used in the flapping equation with nominal parameters and measured values of the other states and controls and the correlation between the homogeneous equation and each forcing function is evaluated. The homogeneous equation was found to be most correlated with controls and body rates, so the coefficients of the controls and body rates that minimize the error between the homogeneous equation and the corresponding forcing functions were identified by regression. The resulting forcing functions are compared with the homogeneous equations in Figure 4. The poor comparison indicates that the model structure is incomplete. The remaining error appeared to be correlated with both the velocity time histories and a bias in the flapping azimuth reference. A mathematical representation of the error in cyclic flapping and feathering due to biases in the blade azimuth references is given in Figure 5. In order to be completely general, separate biases were assumed for the blade azimuths associated with both flapping and feathering measurements. The velocity dependence is most likely related to the quasistatic (Glauert) component of first harmonic inflow so a matrix of coefficients relating these velocities to the homogeneous equation was also added to the model structure. Regression was then used to determine preliminary values for the velocity coefficients and the azimuth biases and the resulting forcing functions are compared with the homogeneous equations in Figure 6. This fit has improved significantly over that of Figure 4 and indicates that the model structure is reasonably close since the resulting parameters identified by the regression are close to the nominal values and are therefore physically meaningful.

System Equations and Parameters

Having determined the modifications to the model structure required to assure consistency with the test data for physically reasonable values of the model parameters, the final step in the system identification process is to identify values for selected parameters. Ten parameters were selected based on the results of the model structure determination process and an understanding of which parameters had well defined values and which were uncertain. The parameters to be identified were the Lock Number (γ), the tip loss factor (B), the inflow time constant (τ), the inflow gain (k) which was related to the deficiency function, biases on the zero azimuth reference for both the flapping and feathering measurements (ψ_1 and ψ_2), and a matrix of four coefficients relating longitudinal and lateral velocity perturbations to the two first harmonic inflow components (k_1, k_2, k_3, k_4). The estimates of the system states ($\hat{a}_{1s}$, $\hat{b}_{1s}$, $\hat{p}_i$, $\hat{q}_i$) for specified values of the parameter set (θ_p) are then given by the following equations.

$$\begin{bmatrix} \ddot{\hat{a}}_{1s} \\ \ddot{\hat{b}}_{1s} \end{bmatrix} + F_1(\theta_p) \begin{bmatrix} \dot{\hat{a}}_{1s} \\ \dot{\hat{b}}_{1s} \end{bmatrix} + F_2(\theta_p) \begin{bmatrix} \hat{a}_{1s} \\ \hat{b}_{1s} \end{bmatrix} = G_1(\theta_p) T^T(\psi_2) \begin{bmatrix} A_{1_m} \\ B_{1_m} \end{bmatrix} + G_3(\theta_p) \begin{bmatrix} p \\ q \end{bmatrix} + G_2(\theta_p) \left(\begin{bmatrix} p_i \\ q_i \end{bmatrix} + \begin{bmatrix} k_1 & k_2 \\ k_3 & k_4 \end{bmatrix} \begin{bmatrix} \mu_x \\ \mu_y \end{bmatrix} \right) \quad (6)$$

$$\begin{bmatrix} \dot{\hat{p}}_i \\ \dot{\hat{q}}_i \end{bmatrix} + F_3(\theta_p) \begin{bmatrix} \hat{p}_i \\ \hat{q}_i \end{bmatrix} = G_4(\theta_p) \left\{ \begin{bmatrix} p \\ q \end{bmatrix} - \begin{bmatrix} 0 & \Omega \\ \Omega & 0 \end{bmatrix} \left(T^T(\psi_2) \begin{bmatrix} A_{1_m} \\ B_{1_m} \end{bmatrix} - \begin{bmatrix} \hat{b}_{1s} \\ \hat{a}_{1s} \end{bmatrix} \right) + \begin{bmatrix} \dot{\hat{a}}_{1s} \\ \dot{\hat{b}}_{1s} \end{bmatrix} \right\}$$

where

$$\theta_p = [\gamma, B, \tau, k]^T$$

As shown in Figure 5, the cyclic flapping measurements (a_{1s_m}, b_{1s_m}) are related to the actual flapping states through the coordinate transformation

$$\begin{bmatrix} a_{1s_m} \\ b_{1s_m} \end{bmatrix} = \begin{bmatrix} \cos\psi_1 & \sin\psi_1 \\ -\sin\psi_1 & \cos\psi_1 \end{bmatrix} \begin{bmatrix} a_{1s} \\ b_{1s} \end{bmatrix} = T(\psi_1) \begin{bmatrix} a_{1s} \\ b_{1s} \end{bmatrix} \quad (7)$$

where ψ_1 represents the bias on the zero azimuth reference point associated with the flapping measurement.

Parameter Identification Methodology

There are three basic methods for parameter identification; the Equation Error method, the Output Error method and the Maximum Likelihood method [Ref. 3]. The simplest is the Equation Error method. This approach finds the parameters, θ_p, of the system that minimize some error function, g, based on the model, given the measurements, z, and inputs, u_c:

$$g(z, \theta_p, u_c) = 0 \quad (8)$$

It is simple to implement if the equations are linear in the parameters, and can also be used for the model structure determination. The Equation Error method requires measurements of all states and controls, and gives biased parameter estimates in the presence of significant measurement noise.

The Output Error method generates system states, x, by integration of the system dynamic equations for a given set of parameter values, θ_p, and a given input history, u_c:

$$\dot{x} = f(x, u_c, \theta_p) \tag{9}$$

In this approach, the parameters are iteratively adjusted by a second order gradient technique to minimize an error function, g, in the outputs, z, the system states, x, the controls, u_c, and the parameters, θ_p:

$$g(x, u_c, z, \theta_p) = 0 \tag{10}$$

This method would give biased estimates if the model structure has significant error. It does not require that all states be measured, however, since it produces state histories from the dynamic model.

The third method for parameter identification is Maximum Likelihood. In this case the state and output equations are combined in an Extended Kalman Filter. The states estimates are then obtained from the equation

$$\dot{\hat{x}} = f(\hat{x}, u_c, \hat{\theta}_p) + K[g(\hat{x}, u_c, z, \hat{\theta}_p)] \tag{11}$$

and the parameters are again iteratively adjusted by a second order gradient method to minimize the error function, $g(\hat{x}, u_c, z, \hat{\theta}_p)$. Maximum Likelihood also does not require all states to be measured. It is the most general identification method since it gives unbiased estimates in the presence of both process and measurement noise. However, the Kalman gains reduce the sensitivity of measurement errors to parameter changes and result in slower convergence.

While the Equation Error method is the simplest, it could not be used in this application because there were two unmeasured states (the first harmonic inflow components). Of the remaining candidates, the Output Error method is the simplest, but its application requires that there is no significant process noise. The model structure validation work had demonstrated that the data could be reasonably well matched with the selected model, indicating a low level of process noise, so the Output Error method was selected.

Application of Output Error Method to Simulated Test Data

The formulation of the Output Error methodology was tested by using the validated model structure (Eq. 6) with selected parameter values to generate output data for the measured input variables (A_1, B_1, p, q). The time histories for these input variables were taken from the longitudinal doublet maneuver at 130 knots and are shown in Figure 4. The Output Error method was then used to estimate the values of the model parameters from the simulated output data. The data was generated with no azimuth bias and no velocity coupling and the model used in the identification problem was configured accordingly. The parameters to be identified were then the Lock Number (γ), the Tip Loss Factor (B), the inflow time constant (τ) and the gain on the inflow forcing function (k). The results of the identification are shown in Figure 7. The problem is highly nonlinear in the selected parameters and fourteen iterations were required to reach convergence on all four parameters. The cost represents the integral of the sum of the squares of the difference between the cyclic flapping output

and control derivatives over a wide range of flight conditions from computer simulations, thereby reducing the number of flight tests required. The potential benefits of system identification technology and the strong probability of success observed in the studies presented at the Bedford Workshop should make further research in this area a strong priority.

Acknowledgements

Advanced Rotorcraft Technology was partially supported by the Rotorcraft Flight Investigations Branch at NASA Ames Research Center in carrying out this research. ART wishes to thank both NASA and the RAE for the opportunity to participate in this Government sponsored collaborative effort.

References

1) Chen, Robert T. N.: *"Effects of Primary Rotor Parameters on Flapping Dynamics"*, NASA TP 1431, January, 1980

2) Gaonkar, Gopal H. and Peters, David A.: *"A Review of Dynamic Inflow and Its Effect on Experimental Correlations"*. Proceedings of the Second Decennial Specialists' Meeting on Rotorcraft Dynamics, NASA Ames Research Center, November 1984.

3. Wang, J.E. and DuVal, R.W., *"Application of Stepwise Regression, Linear Maximum Likelihood Parameter Identification and Extended Kalman Filter/Smoother Programs"*, Final Report for Contract NCC 2-83, Sept. 1981.

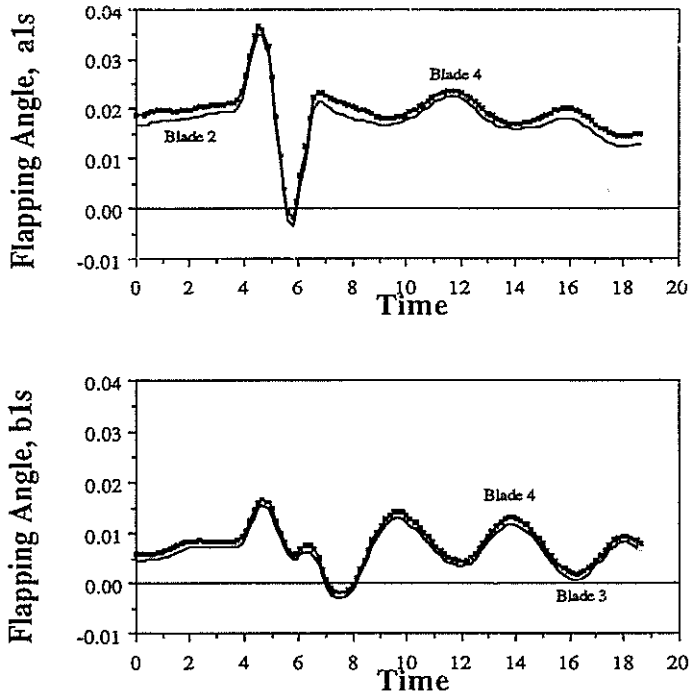

Figure 1: Data Consistency Check – Flapping Angle

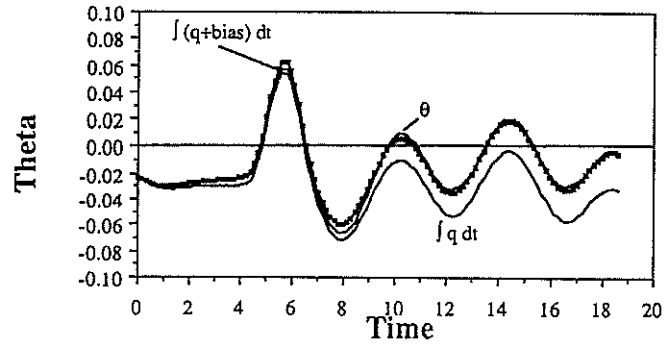

Figure 2: Data Consistency Check – Pitch Angle

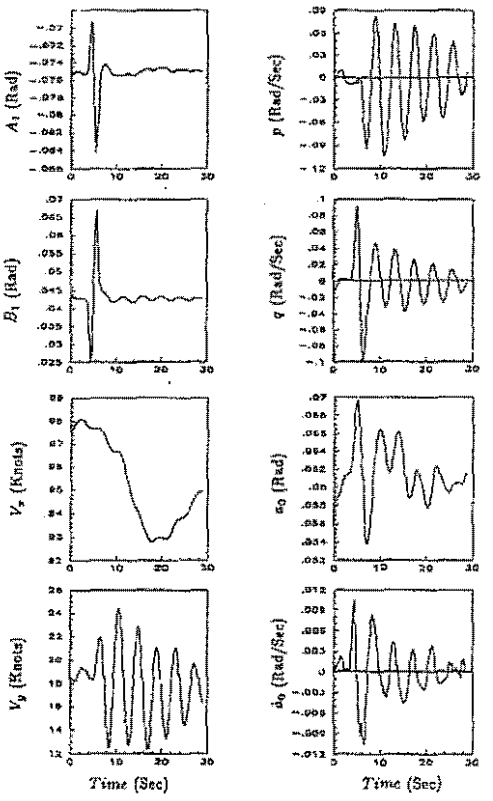

Figure 3: Measured Inputs

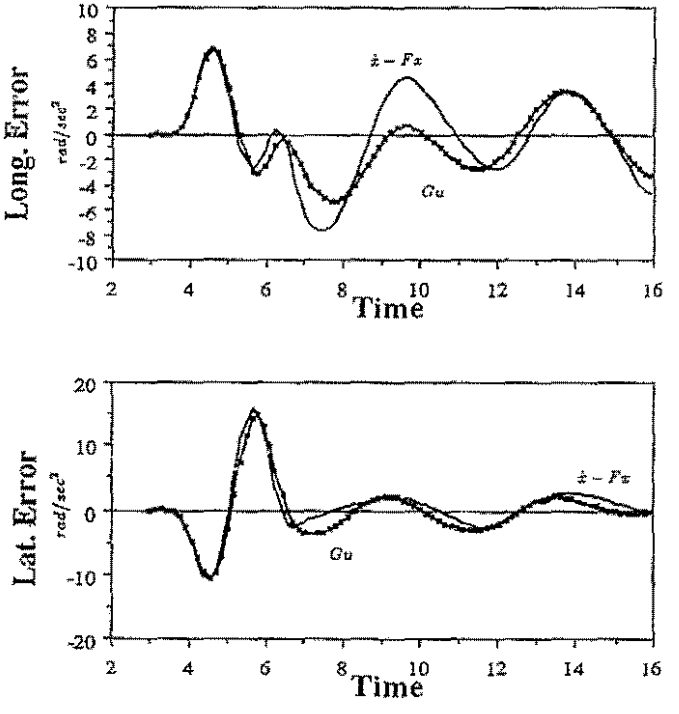

Figure 4: Regression Against Controls and Body Rates

$$\begin{bmatrix} a_{1sm} \\ b_{1sm} \end{bmatrix} = \begin{bmatrix} \cos\ \psi_1 & \sin\ \psi_1 \\ -\sin\ \psi_1 & \cos\ \psi_1 \end{bmatrix} \begin{bmatrix} a_{1s} \\ b_{1s} \end{bmatrix}$$

$$= T(\psi_1) \begin{bmatrix} a_{1s} \\ b_{1s} \end{bmatrix}$$

$$\begin{bmatrix} A_{1m} \\ B_{1m} \end{bmatrix} = \begin{bmatrix} \cos\ \psi_2 & \sin\ \psi_2 \\ -\sin\ \psi_2 & \cos\ \psi_2 \end{bmatrix} \begin{bmatrix} A_1 \\ B_1 \end{bmatrix}$$

$$= T(\psi_2) \begin{bmatrix} A_1 \\ B_1 \end{bmatrix}$$

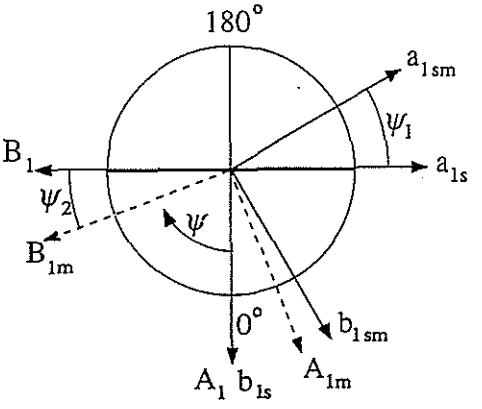

$$\beta = a_0 - a_1 \cos\psi - b_1 \sin\psi$$

$$\theta = A_0 - A_1 \cos\psi - B_1 \sin\psi$$

Figure 5: Measurement Errors

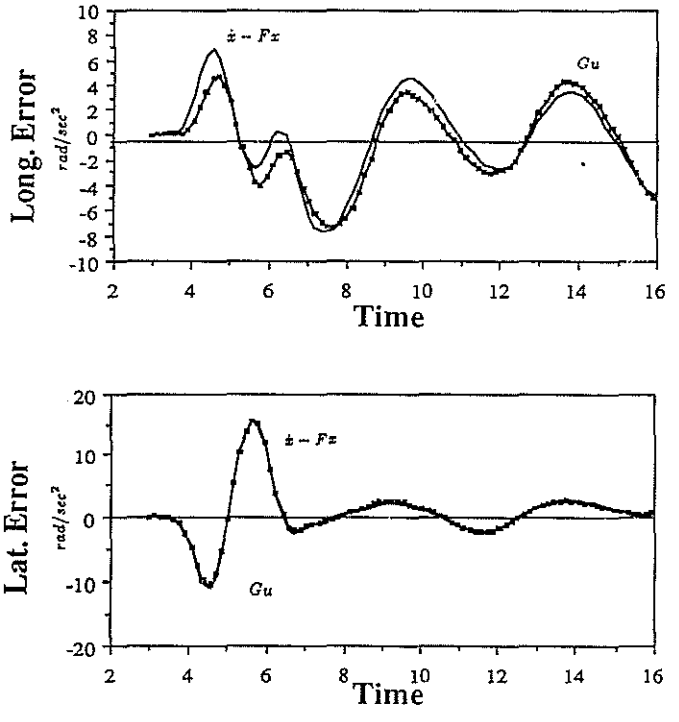

Figure 6: Regression Against Controls, Body Rates, Velocity and Phase Angles

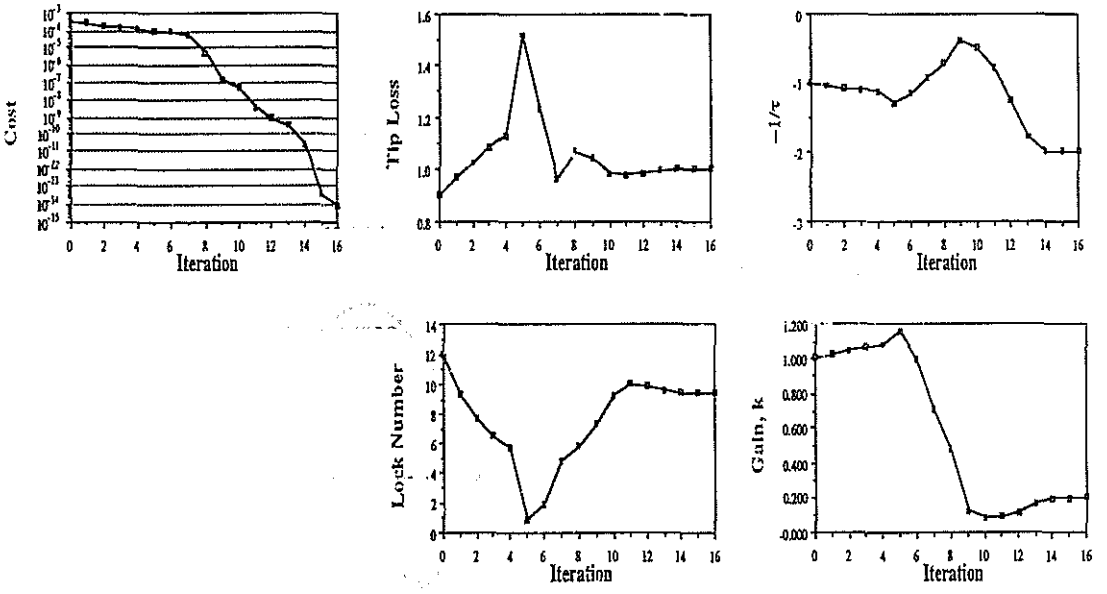

Figure 7: Results of Output Error Identification for Simulated Data (Parameters)

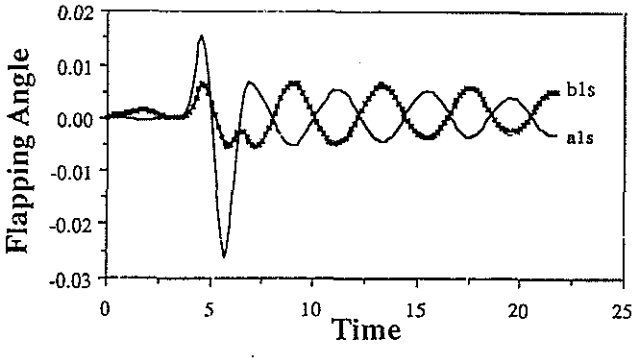

Figure 8: Results of Output Error Identification for Simulated Data (States)

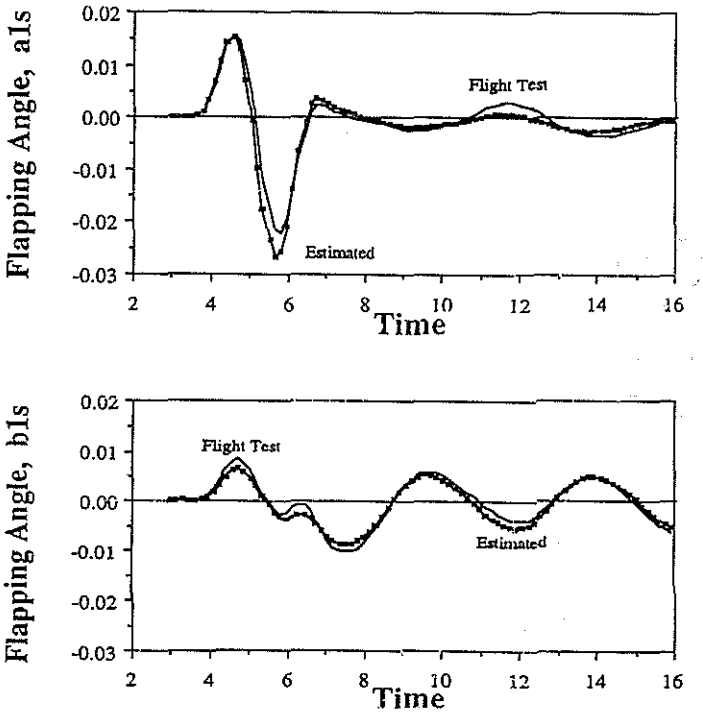

Figure 9: Results of Output Error Identification for Flight Test Data (Longitudinal Maneuver)

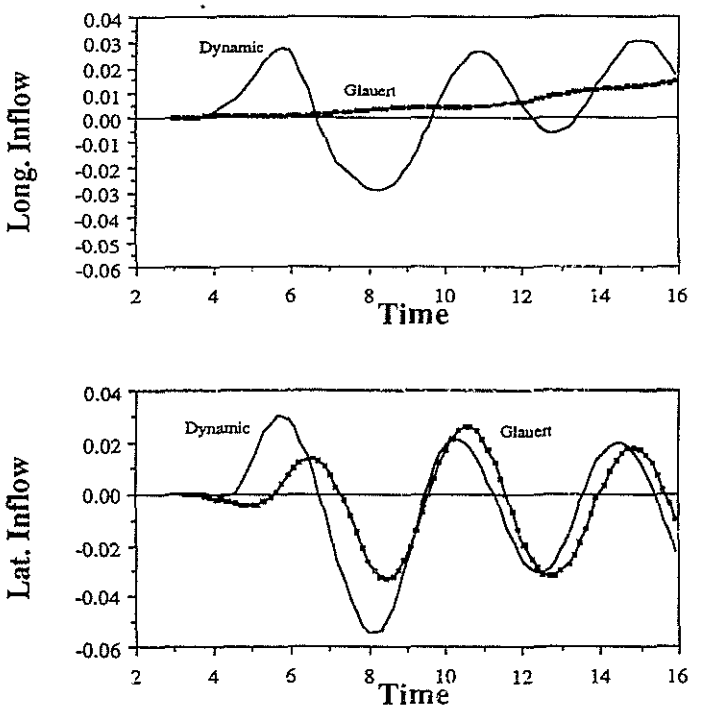

Figure 10: Inflow Effects on Flapping

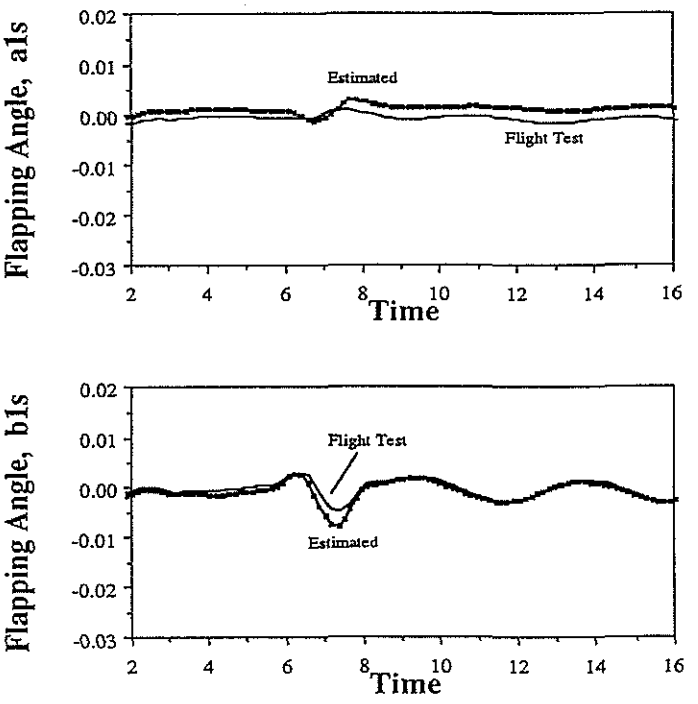

Figure 11: Results of Output Error Identification for Flight Test Data (Lateral Maneuver)

Parameter	Initial	Final	Error %
B	0.9	0.98	0.2
γ	9.5	9.1	0.9
$-1/\tau$	-2.0	-1.1	7.0
k	2.0	0.34	6.5
Ψ_1	0.0	18. 8°	3.3
Ψ_2	0.0	21. 2°	3.1
k_1	0.0	0.042	17.0
k_2	0.0	0.37	2.1
k_3	0.0	-0.23	4.3
k_4	0.0	0.28	2.7

Table 1: Identified Parameters